Title: Quorum-dependent expression of *rsmX* and *rsmY*, small non-coding RNAs, in *Pseudomonas syringae*

Authors' names: Yukiko Nakatsu, Hidenori Matsui, Mikihiro Yamamoto, Yoshiteru Noutoshi, Kazuhiro Toyoda, and Yuki Ichinose*

Affiliations and addresses: Graduate School of Environmental and Life Science, Okayama University, Tsushima-naka 1-1-1, Kita-ku, Okayama 700-8530, Japan

For correspondence: E-mail yuki@okayama-u.ac.jp

Number of figures: 5 including one color figure (Fig. 2)

Number of tables: 3

Word count: 5,571

Supplemental materials: 6 figures and 4 tables

SUMMARY (250 words)

Pseudomonas syringae pathovars are known to produce *N*-acyl-homoserine lactones (AHL) as quorum-sensing molecules. However, many isolates, including *P. syringae* pv. *tomato* DC3000 (*Pto*DC3000), do not produce them. In *P. syringae, psyI*, which encodes an AHL synthase, and *psyR*, which encodes the transcription factor PsyR required for activation of *psyI*, are convergently transcribed. In *P. amygdali* pv. *tabaci* 6605 (*Pta*6605), there is one nucleotide between the stop codons of both *psyI* and *psyR*. However, the canonical stop codon for *psyI* in *Pto*DC3000 was converted to the cysteine codon by one nucleotide deletion, and 23 additional amino acids extended it to a C-terminal end. This resulted in overlapping of the open reading frame (ORF) for *psyI* and *psyR*. On the other hand, stop codons in the *psyR* ORF of *P. syringae* 7 isolates, including pv. *phaseolicola* and pv. *glycinea*, were found. These results indicate that many pathovars of *P. syringae* have genetically lost AHL production ability by the mutation of their responsible genes. To examine whether *Pto*DC3000 modulates the gene expression profile in a population-dependent manner, we carried out microarray analysis using RNAs prepared from low- and high-density cells. We found the expressions of *rsmX* and *rsmY* remarkably activated in high-density cells. The activated expressions of *rsmX* and *rsmY* were confirmed by Northern blot hybridization, but these expressions were abolished in a Δ*gacA* mutant of *Pta*6605. These results indicate that regardless of the ability to produce AHL, *P. syringae* regulates expression of the small noncoding RNAs *rsmX*/*Y* by currently unknown quorum-sensing molecules.

Key words: *N*-acyl-homoserine lactone; Gac two-component system; quorum sensing; *rsmX*; *rsmY*; *Pseudomonas syringae*

1. Introduction

Quorum sensing (QS) is a well-understood mechanism of bacterial cell-cell communication and allows triggering of widespread changes of gene expression in members of the population in a coordinated manner (von Bodman et al., 2003; Ham, 2013; Schuster et al., 2013). QS is mediated by different types of small diffusible molecules, the so-called autoinducers such as *N*-acyl homoserine lactones (AHLs), fatty acid and butyrolactone derivatives, and a variety of peptide structures. Among them, AHLs are the major autoinducers and used by many bacterial species such as the genera *Erwinia*, *Vibrio*, *Pantoea*, *Rhizobium*, and *Pseudomonas* (von Bodman et al., 2003; Ham, 2013; Schuster et al., 2013).

Although *N*-(3-oxo-hexanoly)-L-homoserine lactone (OHHL) and *N*-hexanoly-L-homoserine lactone (HHL) are known to be major QS molecules in *Pseudomonas syringae*, AHL was not detected in many isolates of *P. syringae* (Cha et al., 1998; Elasri et al., 2001). It is not clear why *P. syringae* has AHL-producing and -lacking isolates, and whether AHL-defective isolates of *P. syringae* produce QS molecules besides AHL. In this study, we investigated AHL production and the structure of *psyI*, a gene encoding AHL synthase, and *psyR*, a gene encoding the QS transcription factor, in *P. syringae* pathovars. The AHL synthase gene *psyI* and AHL transcription factor gene *psyR* are also called *ahlI* and *ahlR* in *P. syringae* pv. *syringae* B728a (Quiñones et al., 2004) and *psmI* and *psmR* in *P. syringae* pv. *maculicola* CFBP 10912-9 (Elasri et al., 2001). However, in this paper we used the gene names *psyI* and *psyR* for all AHL synthase genes and transcription factor genes to avoid unnecessary confusion. We found that many isolates, including *P. syringae* pv. *tomato* DC3000 (*Pto*DC3000), do not produce AHLs. Furthermore, mutations of *psyI* and *psyR* are found in many isolates of *P. syringae* that do not produce AHL. These results indicate that some *P. syringae*, including *Pto*DC3000, have genetically lost the ability to produce AHL due to mutation of the corresponding genes.

To examine whether *Pto*DC3000 modulates gene expression profiles in a population-dependent manner, we carried out microarray analysis using RNAs prepared from low- and high-density cells. Most upregulated genes in high-density cells contain *rsmX1* to *rsmX5*, *rsmY*, and *rsmZ* genes. The *rsmX*, *rsmY*, and *rsmZ* are major members of small non-coding regulatory RNAs (sRNAs), and are found in *Pto*DC3000 (Moll et al., 2010). In *Pto*DC3000 *rsmX*, *rsmY*, and *rsmZ* are 112 to 120, 126, and 132 nucleotides in size, respectively (Moll et al., 2010). Small non-coding regulatory RNAs are important components of many physiological and adaptive responses in bacteria (Lapouge et al., 2008; Harfouche et al. 2015). The regulatory mechanisms of small non-coding RNAs were intensively investigated in the biocontrol bacterium *Pseudomonas protegens* CHA0 and the animal pathogen *P. aeruginosa* (Lapouge et al., 2008; Harfouche et al., 2015). In *P. protegens* CHA0, small non-coding RNAs, *rsmX* and *rsmY* express cell density-dependent manner, and capture the translation repressor proteins such as RsmA and RsmE to derepress translation of target mRNAs involved in secondary metabolism and extracellular enzymes. (Kay et al. 2005; Valverde et al. 2004; Lapouge et al., 2008). It is reported that the expression of *rsmX* and *rsmY* in *P. protegens* CHA0 and that of *rsmY* and *rsmZ* in *P. aeruginosa* depend to the GacS/GacA two-component system (Brencic et al. 2009; Humair et al. 2010). Sensor kinase GacS activates and

autophosphorylates by the recognition of yet unidentified signals, and phosphorylates response regulator, GacA. Upon phophorylation, GacA activates the transcription of the target genes, *rsmX*, *rsmY* and *rsmZ* in *P. protegens*. In the promoter of these genes there are conserved sequence elements, the so-called GacA-box or upstream activating sequence (UAS) (Humair et al. 2010). In this study, we found the remarkably upreguated expression of *rsmX* and *rsmY* in high density-cells of *P. syringae*. Based on the evidence, we discuss the involvement of small non-coding RNAs in the system of quorum sensing in *P. syringae*.

2. Materials and methods

2.1. Bacterial strains and growth conditions

The bacterial strains used in this study are listed in Table 1. *Pseudomonas amygdali* pv. *tabaci* 6605 and *P. syringae* pv. *tomato* DC3000 were maintained in King's B (KB) medium at 27°C, and *Escherichia coli* strains were grown at 37°C in Luria-Bertani (LB) medium. *Chromobacterium violaceum* CV026 was grown at 30°C in LB medium with kanamycin at a final concentration of 50 μg/ml (McClean et al., 1997).

2.2. Detection of N-acylhomoserine lactones

Bacterial strains were grown in KB medium with 10 mM $MgCl_2$ for 24 h at 27°C. AHLs extracted with an equal volume of ethyl acetate were detected using C_{18} reversed-phase thin layer chromatography (TLC Silica gel 60, Merck, Darmstadt, Germany) and the biosensor *C. violaceum* CV026 (Taguchi et al., 2006).

2.3. DNA sequence analysis

DNA sequences for *psyI*, *psyR*, and *rpoD* were collected from the Pseudomonas Genome DB site (http://www.pseudomonas-syringae.org). The small non-coding RNAs in *Pta*6605 were searched using each RNA sequence of *Pto*DC3000.

2.4. RNA extraction and microarray analysis

*Pta*6605 and *Pto*DC3000 were cultured overnight in LB supplemented with 10 mM $MgCl_2$ at 27ºC and harvested and suspended in MMMF medium (10 mM mannitol, 10 mM fructose, 50 mM potassium phosphate buffer, 7.6 mM $(NH_4)_2SO_4$, 1.7 mM $MgCl_2$, 1.7 mM NaCl, pH 5.7) to an OD_{600} of 0.01 or 1.0, and further incubated for 3.5 h at 27ºC. Bacteria were harvested by centrifugation, then total RNA was extracted using a TRIzol Max Bacterial RNA Isolation Kit (Thermo Fisher Scientific, Tokyo, Japan), and further purified by treatment with RNase free DNase (Takara, Kusatsu, Japan) and extraction with water-saturated acidic phenol. Total RNA (10 μg) was used for microarray analysis by a microarray system of Hokkaido system Science Co. Ltd.

2.5. Northern blot hybridization

RNA electrophoresis was carried out according to the method of Rio et al. (2010), and Northern blot hybridization was carried out as described (Rio, 2014). One or 0.5 μg of total RNA was denatured in formamide gel-loading buffer (95% deionized formamide, 0.025% bromophenol blue (w/v), 0.025% xylene cyanol FF (w/v)), fractionated by electrophoresis on a denaturing 8% polyacrylamide gel containing 8 M urea in 0.5 × TBE buffer (50 mM Tris base, 50 mM boric acid, 1 mM EDTA) and then blotted onto a nylon membrane filter Hybond-N+ (GE Healthcare, Tokyo, Japan) using Trans-Blot Turbo (Bio-Rad, Hercules, CA). Blotted RNA was confirmed by staining with 0.02% methylene blue in 0.3 M sodium acetate. DIG-labeled oligonucleotide probes (Table 2) of *rsmX2* and *rsmY* of *Pto*DC3000 and *Pta*6605 were prepared using terminal deoxynucleotidyl transferase (Takara) and DIG-11-ddUTP (Sigma-Aldrich, Darmstadt, Germany). Hybridization was performed at 60ºC overnight in a hybridization mix (50% formamide, 5 × SSC, 3 × Denhardt's solution, 200 μg/mL herring testis carrier DNA, 0.1% SDS) with a DNA probe. Final washes were at 60ºC in a solution containing 0.1 × SSC and 1% SDS. Hybridized RNAs were detected with anti-DIG antibody conjugated with alkaline phosphatase (Roche Diagnostics, Basel, Switzerland), and its chemiluminescent substrate, CDP-star (Thermo Fisher Scientific, Tokyo, Japan). Chemiluminescent was detected using ChemiDoc Touch (Bio-Rad, Hercules, CA, USA).

3. Results

3.1. Production of AHL in Pseudomonas syringae

AHL production of different pathovars of *P. syringae* was investigated. The isolates investigated are listed in Table 1 and Table S1. Among the isolates of *P. syringae*, AHL production was observed in only *P. amygdali* pv. *tabaci* 6605 (*Pta*6605), pv. *tabaci* 11528, and pv. *syringae* B728a, as previously reported (Taguchi et al., 2006; Cheng et al., 2016; Quiñones et al., 2004); however, there are fewer reports of AHL production in other *P. syringae* strains. Using different isolates of *P. syringae* (on a recent taxonomy, they were divided into *P. amygdali*, *P. savastanoi*, and *P. syringae*, Table 1, Gomila et al., 2017), we investigated whether independent isolates produce AHL using a bioassay with *Chromobacterium violaceum* CV026, as shown in Fig. S1. AHL was produced only by *P. amygdali* pv. *tabaci* 6605, 11528, and pv. *syringae* B728a; the other isolates did not produce detectable AHL.

3.2. Gene structure of psyI and psyR in P. syringae

The *psyI* and *psyR* genes of several isolates of *P. syringae* including genes registered in the *Pseudomonas* database were analyzed (Figs. S2, S3). In *P. syringae*, *psyI* and *psyR* are convergently transcribed, and there is one nucleotide between both stop codons in *Pta*6605. The DNA sequences for *psyI* and *psyR* are well conserved. However, the canonical stop codon, TGA for *psyI* in *Pto*DC3000, pv. *tomato* T1, and pv. *maculicola* H7608, is converted to the valine codon GTC by one nucleotide deletion, and an additional 22 amino acids

extend to a C-terminal end. This resulted in overlapping of the 3'-end of open reading frames (ORF) for both *psyI* and *psyR* (Fig. S4). The overlapping structure might interfere with their transcription and translation. On the other hand, there is a mutational stop codon in the 9th amino acid in *psyR* ORF in *P. savastanoi* pv. *phaseolicola* (*Pph*) 1448A, *Pph*Y5_2, pv. *maculicola* KN91, *P. amygdali* pv. *mellea* N6801, and three isolates of *P. savastanoi* pv. *glycinea* (Fig. S5). Furthermore, three isolates of *P. savastanoi* pv. *glycinea* have one nucleotide deletion at 120 nucleotides from the translation start codon, which resulted in a serious frame shift with additional seven stop codons in their ORFs, and the ORFs are completely destroyed (Fig. S5).

In Fig. 1, we summarized the result of AHL production, schematic depiction of *psyI* and *psyR*, with phylogenetic analysis of these strains. The phylogenetic tree was generated using the UPGMA method using *rpoD* sequences by Genetyx version 19.0.0 (Genetyx, Tokyo, Japan). From this result we found that the mutation of *psyI* or *psyR* occurred in phylogenetically related bacteria, indicating that each isolate of *P. syringae* has evolved to lose the AHL production.

3.3. Gene expression profiles of low- and high-density cells in P. syringae pv. tomato DC3000

To confirm bacterial cell density-dependent gene expression in *Pto*DC3000, we carried out microarray analysis using RNAs prepared from low- (OD_{600} = 0.01) and high-density (OD_{600} = 1.0) cells. The result is shown in Table S2: the expressions of 303 genes were up-regulated (Table S3), and 101 genes were down-regulated in the high-density cells (Table S4). Among the up-regulated genes, remarkably high expression was observed in small non-coding regulatory RNAs, i.e., five members of *rsmX* (*rsmX1-X5*), *rsmY,* and *rsmZ* (Fig. 2 and Table 3, Moll et al., 2010). Expression of *rsmX1-5* and *rsmY* was increased 9- to 56-fold in high-density cells, whereas that of *rsmZ* increased 2.6-fold. A significant level of *rsmY* expression was also observed in low-density cells, but it remarkably upregulated in high-density cells. On the other hand, there are also down-regulated genes in the high-density condition as indicated blue dots in Fig. 2. There are significant number of flagella-related genes in the genes which remarkably down-regulated (Table S4), indicating that flagella motility decreases in high-density condition. However, the relationship of most genes to QS is not clear.

3.4. rsmX, rsmY, and rsmZ genes in Pta6605

Each ortholog of *rsmX* (*rsmX1-X5*), *rsmY*, and *rsmZ* was identified in *Pta*6605 draft sequences (Fig. S6). The upstream activating sequences (UAS, Humair et al., 2010) were well conserved in the upstream promoter regions of five orthologs of *rsmX* and *rsmY.* However, it was less conserved in *rsmZ.* All *rsmX*, *rsmY*, and *rsmZ* possessed many GGA motifs in the transcribed regions. At the 3' end of five *rsmX* and *rsmY* genes, there were sequences to form a stem-loop structure, which functions as a ρ-independent terminator as found in *Pto*DC3000 (Moll et al., 2010).

179 *3.5. Expression of rsmX2 and rsmY in PtoDC3000 and Pta6605*

180 Enhanced expression of small non-coding RNAs was also investigated by Northern blot hybridization in
181 *Pto*DC3000 and *Pta*6605. Total RNAs prepared from low- (OD_{600} = 0.01) and high-density (OD_{600} = 1.0) cells
182 of the AHL production–defective bacterium *Pto*DC3000 wild-type (WT) and the AHL-producing bacterium
183 *Pta*6605. The microarray results showed that the expression of *rsmX2* was the strongest among the *rsmX* family
184 in the high-density cells. Furthermore, *rsmY* was the strongest sRNA in high-density cells (Table 3). Therefore,
185 we carried out Northern blot hybridization to detect *rsmX2* and *rsmY* in a low- and high-density cell conditions.
186 In *Pto*DC3000, the signal corresponding to *rsmX2* was detected in only high-density cells but not in low-density
187 cells (Fig. 3A). The signal for *rsmY* was also strongly detected in high-density cells but was only weakly
188 detected in low-density cells (Fig. 3B). We also investigated transcripts for *rsmX2* and *rsmY* in *Pta*6605. The
189 results were almost identical to the case of *Pto*DC3000: there were almost no signals for *rsmX2* and *rsmY* in
190 low-density cells, whereas significant levels of transcripts for *rsmX2* and *rsmY* were observed in high-density
191 cells (Fig. 3CD).

192

193 *3.6. Expression of rsmX2 and rsmY in Pta6605 Δ*gacA*

194 Because it was reported that the expression of small non-coding RNAs is dependent on the GacS/GacA two-
195 component system in *P. fluorescens* (*P. protegens*) CHA0 and *P. aeruginosa* (Kay et al., 2005, 2006; Valverde
196 et al., 2003), we investigated the expression of *rsmX2* and *rsmY* in *Pta*6605 using a previously generated Δ*gacA*
197 mutant (Marutani et al., 2008). As shown in Fig, 4, the expression of *rsmX2* was not detected, and that of *rsmY*
198 was only weakly detected and not significantly increased in high-density cells of the Δ*gacA* mutant.

199

200 *3.7. Expression of rsmX2 and rsmY in Pta6605 ΔpsyI, ΔpsyR, and ΔaefR*

201 Because it is known that AHLs are major QS molecules in *P. syringae*, we investigated the expression of *rsmX2*
202 and *rsmY* in both WT and previously generated QS-defective mutants such as Δ*psyI* and Δ*psyR* mutant strains of
203 *Pta*6605 (Taguchi et al., 2006; Ichinose et al., 2018). As shown in Fig. 5, the expressions of *rsmX2* and *rsmY* in
204 these mutant strains were almost identical to those of the WT strain. It is also known that AHL production in the
205 Δ*aefR* mutant of *Pta*6605 was also abolished (Kawakita et al., 2012). The expressions of *rsmX2* and *rsmY* were
206 also induced in high-density cells in these mutants. However, the expression of *rsmX2* and *rsmY* in low-density
207 cells was stronger in the Δ*aefR* mutant than in the WT strain. Furthermore, we investigated the effect of
208 exogenous application of AHL (at 10 μM final concentration of each HHL and OHHL) on the expression of
209 *rsmX2* in the AHL-production defective mutant *Pta*6605 Δ*psyI* and *Pto*DC3000 WT strains. The expression of
210 *rsmX2* was evaluated as a β-galactosidase activity which derived from *rsmX2* promoter. We found that the β-
211 galactosidase activity derived from *rsmX2* promoter increased in a bacterial density-dependent manner and

212 regardless of the existence of AHL in these strains (data not shown). These results clearly showed that AHL did
213 not affect the expression of *rsmX2*.
214
215 **4. Discussion**
216 *4.1. Decline in AHL production capacity*
217 Although AHL production was reported previously in some strains of *P. syringae* (Cha et al., 1998; Elasri et al.,
218 2001), this study revealed that AHL-producing bacteria are not majority. In this study, we investigated the AHL
219 production by biosensor bacteria along with genetic information on AHL synthases (*psyI*) and AHL
220 transcription factors (*psyR*) of several isolates of *P. syringae.* As a result of the investigation, we found that
221 many isolates of *P. syringae* not only abolished AHL production, but also mutated AHL production-related
222 genes. Interestingly, *P. syringae* isolates belonging to the same clade have the same or similar gene structures of
223 *psyI* and *psyR* (Fig. 1). Each isolate belonging to the same clade as *Pph*1448A has substituted stop codon at the
224 position of the 9th amino acid of *psyR*. Furthermore, three isolates of *P. savastanoi* pv. *glycinea* in this clade not
225 only have the same substitution at the 9th amino acid, but also one nucleotide deletion with a serious frame shift.
226 Overlapping of ORF for both *psyI* and *psyR* occurred in all isolates of the clade to which *Pto*DC3000 belongs.
227 This suggests that the mutation of *psyI* and *psyR* genes occurred with differentiation of *P. syringae* pathovars. It
228 means that ancestors of *P. syringae* had produced AHL, but that most *P. syringae* strains had abolished it
229 because AHL production might become inconvenient for successful infection by the pathogenic bacteria. Thus,
230 most *P. syringae* might have abandoned production of AHL by the introduction of a mutation in *psyI* or *psyR*
231 genes.
232
233 *4.2. Effect of AHL on plant physiology*
234 Why did many isolates of *P. syringae* abandon the ability to produce AHL? Although AHLs are a
235 communication tool used by individual bacterial cells to monitor the population density and coordinate gene
236 expression profiles, AHLs are also recognized by plants and animals (Hartmann and Schikora, 2012; Teplitski et
237 al., 2011). Accumulated reports suggest that AHL induces plant growth and plant defense responses (Schenk
238 and Schikora, 2015). The effect of AHLs varies depending on the type of AHL and plant species. However,
239 HHL-treated tomatoes accumulated salicylic acid and activated the transcription of *PR-1* and *chitinase* genes
240 (Schuhegger et al., 2006), suggesting that AHLs are undesired molecules in tomato infection by *Pto*DC3000.
241 How do plants recognize AHL? In *Arabidopsis*, OHHL and *N*-3-oxo-octanoil-homoserine lactone
242 (OOHL) induced root elongation at 1–10 μM concentrations (Liu et al., 2012). In this AHL-mediated elongation
243 of *Arabidopsis* roots, GCR1, a G-protein-coupled receptor, and GPA1, the sole canonical Gα subunit, are
244 involved (Liu et al., 2012). Furthermore, AHL was amidolyzed by a plant-derived fatty acid amide hydrolase to
245 yield L-homoserine in *Arabidopsis* (Palmer et al., 2014). The accumulation of L-homoserine promotes plant

246 growth at low concentrations by stimulating transpiration, while higher concentrations inhibit growth by
247 stimulating ethylene production (Palmer et al., 2014).
248
249 *4.3. Gac/Rsm system controls QS-dependent bacterial phenotype*
250 The expressions of *rsmX2* and *rsmY* are activated in high density-cells of *Pto*DC3000 and *Pta*6605 regardless
251 the production of AHL. The expression of *rsmX2* and *rsmY* was investigated using multiple mutant strains of
252 *Pta*6605. The Δ*gacA* mutant completely abolished the expression of *rsmX2,* and that of *rsmY* was remarkably
253 reduced (Fig. 4). The low level of *rsmY* was expressed regardless of bacterial cell density, indicating that *rsmY*
254 is under the control of an expression system other than the GacS/A two-component system. The expression of
255 *rsmX2* and *rsmY* was not changed in the Δ*psyI* and Δ*psyR* mutant strains of *Pta*6605 (Fig. 5). Furthermore,
256 exogenous application of AHL in *Pta*6605 Δ*psyI* and *Pto*DC3000 WT did not affect the expression of *rsmX2*
257 (data not shown). This result indicates that the Rsm-mediated gene expression pathway might control the AHL-
258 mediated gene expression pathway.
259 Previously, we investigated the phenotype of a Δ*gacA* mutant strain in *Pta*6605 (Marutani et al., 2008).
260 The Δ*gacA* mutant lost swarming motility and production of fluorescent pigment, and remarkably reduced AHL
261 production. We speculated that the swarming motility and pigment production were regulated via a Gac/Rsm
262 pathway because the addition of a mixture of HHL and OHHL to *gac*-defective mutants did not restore these
263 phenotypes (Marutani et al., 2008). The Δ*gacA* mutant also had reduced expression levels of *algT* and *hrp*
264 genes, adhesion, and exopolysaccharide production. It is possible that these phenotypes might be also regulated
265 via a Gac/Rsm signal pathway.
266 Kong et al. (2012) overexpressed *rsmA* of *P. aeruginosa* in *P. syringae* pv. *phaseolicola* NPS3121, pv.
267 *syringae* B728a and BR2R, and found that *rsmA*-overexpressers abolished production of phytotoxins such as
268 phaseolotoxin, syringomycin, and tabtoxin. Furthermore, these strains diminished the production of protease
269 and pyoverdine as well as swarming motility, and remarkably reduced the ability to cause disease in their host
270 plants (Kong et al., 2012). These results indicated that RsmA repressed the translation of virulence-related
271 mRNA. In *Pto*DC3000, five members of RsmA/CsrA are known (Ferreiro et al., 2018). Ferreiro et al. (2018)
272 generated deletion mutants for the most conserved *csrA1*, *csrA2*, and *csrA3*, and investigated the possible
273 involvement of CsrA1, CsrA2, and CsrA3 in virulence-related traits. Thus, Ferreiro et al. (2018) found that the
274 Δ*csrA3* enhanced alginate production accompanying activation of the alginate biosynthesis gene *algD*,
275 swarming motility, and *hrp* gene expression, suggesting that CsrA3 plays a pivotal role in bacterial virulence.
276 Very recently it was reported that motility, expression of type III secretion-related genes, and biofilm
277 formation were regulated by both the Gac/Rsm regulatory system and cyclic di-guanosine monophosphate (c-di-
278 GMP) (Bhagirath et al., 2018). High levels of c-di-GMP were reported to correlate with evasion of plant
279 immunity in *Pseudomonas* by inhibiting flagellin synthesis, although the in planta growth of *Pto*DC3000 in

280 which c-di-GMP is high was drastically reduced after the spray inoculation by impaired migration into the
281 apoplast (Pfeilmeier et al., 2016). Thus, there is a link between c-di-GMP and *rsmZ* in the regulation of the
282 motile-sessile switch in *P. aeruginosa* and *P. fluorescens* (Petrova et al., 2014). A mutant for GcbA, a
283 diguanylate cyclase (GDC), had enhanced motility but reduced initial surface attachment activity and *rsmZ*
284 expression. On the contrary, a *gcbA*-overexpression strain had reduced motility, but initial surface attachment
285 activity and *rsmZ* expression were activated. Furthermore, changes in the above activities in the Δ*gcbA* mutant
286 were restored by the overexpression of *rsmZ* (Petrova et al., 2014). These results indicate that the functions of
287 GcbA are at least partially dependent on *rsmZ* and that c-di-GMP potentially contributes to the regulation of
288 *rsmZ* abundance (Petrova et al., 2014).
289 The expressions of *rsmX2* and *rsmY* were cell density–dependent (Fig. 3). However, the signal(s) that
290 activate the Gac two-component system were not clear. Besides AHL, *P. syringae* should produce and secrete
291 novel signal(s) to recognize bacterial population by themselves. Further investigation is necessary.
292
293 **Conflicts of Interest:** The authors declare no conflict of interest.
294
295 **Acknowledgements**
296 This work was supported in part by Grants-in-Aid for Scientific Research (No. 15H04458) from the Ministry of
297 Education, Culture, Sports, Science and Technology of Japan.
298
299 **References**
300 Bhagirath, A.Y., Somayajula, D., Li, Y., Duan, K. 2018. CmpX affects virulence in *Pseudomonas aeruginosa*
301 through the Gac/Rsm signaling pathway and by modulating c-di-GMP levels. J. Membr. Biol. 251, 35-49.
302 Brencic, A., McFarland, K.A., McManus, H.R., Castang, S., Mogno, I., Dove, S.L., Lory, S. 2009. The
303 GacS/GacA signal transduction system of *Pseudomonas aeruginosa* acts exclusively through its control
304 over the transcription of the RsmY and RsmZ regulatory small RNAs. Mol. Microbiol. 73, 434-445.
305 Cha, C., Gao, P., Chen, Y.-C., Shaw, P.D. Farrand, S.K. 1998. Production of acyl-homoserine lactone quorum-
306 sensing signals by Gram-negative plant-associated bacteria. Mol. Plant-Microbe Interact. 11, 1119-1129.
307 Cheng, F., Ma, A., Zhuang, G., Fray, R.G. 2016. Exogenous *N*-acyl-homoserine lactones enhance the
308 expression of flagella of *Pseudomonas syringae* and activate defence responses in plants. Mol. Plant Pathol.
309 19, 104-115.
310 Elasri, M., Delorme, S., Lemanceau, P., Stewart, G., Laue, B., Glickmann, E., Oger, P.M., Dessaux, Y. 2001.
311 Acyl-homoserine lactone production is more common among plant-associated *Pseudomonas* spp. than
312 among soilborne *Pseudomonas* spp. Appl. Environ. Microbiol. 67, 1198-1209.

313 Ferreiro, M.-D., Nogales, J., Farias, G.A., Olmedilla, A., Sanjuán J., Gallegos, M.T. 2018. Multiple CsrA
314 proteins control key virulence traits in *Pseudomonas syringae* pv. *tomato* DC3000. Mol. Plant-Microbe Int.
315 31, 525-536
316 Gomila, M., Busquets, A., Mulet, M., García-Valdés, E., Lalucat, J. 2017. Clarification of taxonomic status
317 within the *Pseudomonas syringae* species group based on a phylogenomic analysis. Front. Microbiol. 8,
318 2422.
319 Ham, J.H. 2013. Intercellular and intracellular signalling systems that globally control the expression of
320 virulence genes in plant pathogenic bacteria. Mol. Plant Pathol. 14, 308-322.
321 Harfouche, L., Haichar, F.E.Z., Achouak, W. 2015. Small regulatory RNAs and the fine-tuning of plant–
322 bacteria interactions. New Phytologist 206, 98-106.
323 Hartmann, A., Schikora, A. 2012. Quorum sensing of bacteria and trans-kingdom interactions of *N*-acyl
324 homoserine lactones with eukaryotes. J. Chem. Ecol. 38, 704-713.
325 Humair, B., Wackwitz, B., Haas, D. 2010. GacA-controlled activation of promoters for small RNA genes in
326 *Pseudomonas fluorescens*. Appl. Environ. Microbiol. 76, 1497-1506.
327 Ichinose, Y., Tasaka, Y., Yamamoto, S., Inoue, Y., Takata, M., Nakatsu, Y., Taguchi, F., Yamamoto, M.,
328 Toyoda, K., Noutoshi, Y., Matsui, H. PsyR, a transcriptional regulator in quorum sensing system, binds *lux*
329 box-like sequence in *psyI* promoter without AHL and activates its transcription with AHL in *Pseudomonas*
330 *syringae* pv. *tabaci* 6605. Submitted.
331 Kawakita, Y., Taguchi, F., Inagaki, Y., Toyoda, K., Shiraishi, T., Ichinose, Y. 2012. Characterization of each
332 *aefR* and *mexT* mutant in *Pseudomonas syringae* pv. *tabaci* 6605. Mol. Genet. Genomics 287, 473-484.
333 Kay, E., Dubuis, C., Haas, D. 2005. Three small RNAs jointly ensure secondary metabolism and biocontrol in
334 *Pseudomonas fluorescens* CHA0. Proc. Natl. Acad. Sci. USA 102, 17136-17141.
335 Kay, E., Humair, B., Dénervaud, V., Riedel, K., Spahr, S., Eberl, L., Valverde, C., Haas, D. 2006. Two GacA-
336 dependent small RNAs modulate the quorum sensing response in *Pseudomonas aeruginosa*. J. Bacteriol.
337 188, 6026–6033.
338 Kong, H.S., Roberts, D.P., Patterson, C.D., Kuehne, S.A., Heeb, S., Lakshman, D.K., Lydon, J. 2012. Effect of
339 overexpressing *rsmA* from *Pseudomonas aeruginosa* on virulence of select phytotoxin-producing strains of
340 *P. syringae*. Phytopatholgy 102, 575 – 587.
341 Lapouge, K., Schubert, M., Allain, F.H., Haas, D. 2008. Gac/Rsm signal transduction pathway of γ-
342 proteobacteria: from RNA recognition to regulation of social behaviour. Mol. Microbiol. 67, 241-253.
343 Liu, F., Bian, Z., Jia, Z., Zhao, Q., Song, S. 2012. The GCR1 and GPA1 participate in promotion of *Arabidopsis*
344 primary root elongation induced by *N*-acyl-homoserine lactones, the bacterial quorum sensing signals. Mol.
345 Plant-Microbe Interact. 25, 677-683.

346 Marutani, M., Taguchi, F., Ogawa, Y., Hossain, M.M., Inagaki, Y., Toyoda, K., Shiraishi, T., Ichinose, Y. 2008.
347 Gac two-component system in *Pseudomonas syringae* pv. *tabaci* is required for virulence but not for
348 hypersensitive reaction. Mol. Genet. Genomics 279, 313-322.
349 McClean, K.H., Winson, M.K., Fish, L., Taylor, A., Chhabra, S.R., Camara, M., Daykin, M., Lamb, J.H., Swift,
350 S., Bycroft, B.W., Stewart, G.S., Williams, P. 1997. Quorum sensing and *Chromobacterium violaceum*:
351 exploitation of violacein production and inhibition for the detection of *N*-acylhomoserine lactones.
352 Microbiology 143, 3703-3711.
353 Moll, S., Schneider, D.J., Stodghill, P., Myers, C.R., Cartinhour, S.W., Filiatrault, M.J. 2010. Construction of an
354 *rsmX* co-variance model and identification of five *rsmX* non-coding RNAs in *Pseudomonas syringae* pv.
355 *tomato* DC3000. RNA Biol. 7, 508-516.
356 Palmer, A.G., Senechal, A.C., Mukherjee, A., Ané, J.-M., Blackwell, H.E. 2014. Plant responses to bacterial *N*-
357 acyl L-homoserine lactones are dependent on enzymatic degradation to L-homoserine. ACS Chem. Biol. 9,
358 1834–1845.
359 Petrova, O.E., Cherny, K.E., Sauer, K. 2014. The *Pseudomonas aeruginosa* diguanylate cyclase GcbA, a
360 homolog of *P. fluorescens* GcbA, promotes initial attachment to surfaces, but not biofilm formation, via
361 regulation of motility. J. Bacteriol. 196, 2827-2841.
362 Pfeilmeier, S., Saur, I.M., Rathjen, J.P., Zipfel, C., Malone, J.G. 2016. High levels of cyclic-di-GMP in plant-
363 associated *Pseudomonas* correlate with evasion of plant immunity. Mol. Plant Pathol. 17, 521-531.
364 Quiñones, B., Pujol, C.J., Lindow, S.E. 2004. Regulation of AHL production and its contribution to epiphytic
365 fitness in *Pseudomonas syringae*. Mol. Plant-Microbe Interact. 17, 521-531.
366 Rio, D.C. 2014. Northern blots for small RNAs and microRNAs. Cold Spring Harb. Protoc. 2014,
367 pdb.prot080838-pdb.prot080838.
368 Rio, D.C., Ares, M., Hannon, G.J., Nilsen, T.W. 2010. Polyacrylamide gel electrophoresis of RNA. Cold Spring
369 Harb. Protoc. 2010, pdb.prot5444-pdb.prot5444.
370 Schenk, S.T., Schikora, A. 2015. AHL-priming functions via oxylipin and salicylic acid. Front. Plant Sci. 5,
371 784.
372 Schuhegger, R., Ihring, A., Gantner, S., Bahnweg, G., Knappe, C., Vogg, G., Hutzler, P., Schmid, M., Van
373 Breusegem, F., Eberl, L., Hartmann, A., Langebartels, C. 2006. Induction of systemic resistance in tomato
374 by *N*-acyl-L- homoserine lactone-producing rhizosphere bacteria. Plant Cell Environ. 29, 909-918.
375 Schuster, M., Sexton, D.J., Diggle, S.P., Greenberg, E.P. 2013. Acyl-homoserine lactone quorum sensing: from
376 evolution to application. Annu. Rev. Microbiol. 67, 43-63.
377 Teplitski, M., Mathesius, U., Rumbaugh, K.P. 2011. Perception and degradation of *N*-acyl homoserine lactone
378 quorum sensing signals by mammalian and plant cells. Chem. Rev. 111, 100-116.
379 Taguchi, F., Ogawa, Y., Takeuchi, K., Suzuki, T., Toyoda, K., Shiraishi, T., Ichinose, Y. 2006. A homologue of
380 the 3-oxoacyl-(acyl carrier protein) synthase III gene located in the glycosylation island of *Pseudomonas*

syringae pv. tabaci regulates virulence factors via *N*-acyl homoserine lactone and fatty acid synthesis. J. Bacteriol. 188, 8376-8384.

Valverde, C., Heeb, S., Keel, C., Haas, D. 2003. RsmY, a small regulatory RNA, is required in concert with RsmZ for GacA-dependent expression of biocontrol traits in *Pseudomonas fluorescens* CHA0. Mol. Microbiol. 50, 1361-1379.

Valverde, C., Lindell, M., Wagner, E.G., Haas, D. 2004. A repeated GGA motif is critical for the activity and stability of the riboregulator *RsmY* of *Pseudomonas fluorescens*. J. Biol. Chem. 279:25066-25074.

von Bodman, S.B., Bauer, W.D., Coplin, D.L. 2003. Quorum sensing in plant-pathogenic bacteria. Annu. Rev. Phytopathol. 41, 455-482.

Figure legends

Fig. 1. Structure of quorum sensing genes, *psyI* and *psyR*, and production of *N*-acylhomoserine lactones in *Pseudomonas syringae* pathovars and isolates.

A phylogenetic tree of pathovars and isolates of *P. syringae* was constructed based on the sequence of *rpoD*. A gene for AHL synthase, *psyI*, and a gene for a transcriptional regulator, *psyR*, are transcribed convergently. Overlapping regions of two arrows indicate overlapping of two open reading frames. The dark portion in arrows of *psyR* indicates an untranslatable sequence by the stop codon(s) generated by the nucleotide substitution(s). The right column of AHL indicates the experimental result of AHL production. AHL detection is indicated as plus (+) and minus (-). NT: not tested.

Fig. 2 Result of microarray analysis.

The open source R software (R version 3.2.5, http://www.r-project.org/) was used for microarray analysis and visualization. Genes expressed in *P. syringae* pv. *tomato* DC3000 at high cell density (OD_{600} = 1.0) and at low cell density (OD_{600} = 0.01) were plotted. Each dot represents individual level of gene expression. Red dots and blue dots indicate the genes expressed more than twice as much and less than half as much in high cell density conditions, respectively, whereas grey dots indicate the genes expressed more than half and less than twice as much. Five *rsmX*, *rsmY* and *rsmZ* genes are shown.

Fig. 3 Northern blot hybridization of *rsmX2* (A and C) and *rsmY* (B and D) of *Pto*DC3000 (A and B) and *Pta*6605 (C and D).

In each set of experiments, the methylene blue-stained membrane is shown on the left, and the corresponding hybridization result is shown on the right. Total RNAs (1 μg of *Pto*DC3000 and 0.5 μg of *Pta*6605) prepared from low-density cells (lane L, OD_{600} = 0.01) and high-density cells (lane H, OD_{600} = 1.0) were used for Northern blot hybridization. DIG-labeled oligonucleotides, Pto-rsmX2-R and Pto-rsmY-R, were used as hybridization probes for *Pto*DC3000, and Pta-rsmX2-R and Pta-rsmY-R for *Pta*6605, respectively.

Fig. 4 Northern blot hybridization of *rsmX2* (A and C) and *rsmY* (B and D) of *Pta*6605 WT (A and B) and *Pta*6605Δ*gacA* (C and D).

In each set of experiments, the methylene blue-stained membrane is shown on the left, and the corresponding hybridization result is shown on the right. Total RNAs (1 μg of *Pta*6605) prepared from low-density cells (lane L, OD_{600} = 0.01) and high-density cells (lane H, OD_{600} = 1.0) were used for Northern blot hybridization. DIG-labeled oligonucleotides, Pta-rsmX2-R, and Pta-rsmY-R were used as hybridization probes for *Pta*6605.

Fig. 5 Northern blot hybridization of *rsmX2* (A, C, E and G) and *rsmY* (B, D, F and H) of *Pta*6605 WT (A and B), *Pta*6605Δ*psyI* (C and D), *Pta*6605Δ*psyR* (E and F), and *Pta*6605Δ*aefR* (G and H).
In each set of experiments, the methylene blue-stained membrane is shown on the left, and the corresponding hybridization result is shown on the right. Total RNAs (1 µg of *Pta*6605) prepared from low-density cells (lane L, OD_{600} = 0.01) and high-density cells (lane H, OD_{600} = 1.0) were used for Northern blot hybridization. DIG-labeled oligonucleotides, Pta-rsmX2-R, and Pta-rsmY-R were used as hybridization probes for *Pta*6605.

SUPPPORTING INFORMATION

Additional Supporting Information may be found in the online version of this article at the publisher's website:

Fig. S1 AHL production in different *P. syringae* isolates.
Ethyl acetate extract from 2 ml of bacterial culture from each bacterium was spotted on TLC plates. Red marks indicate that DNA sequence analysis was also done as shown in Fig. 1.

Fig. S2 Amino acid alignment of PsyI protein of different isolates of *P. syringae*.
Asterisks and dots below the sequences indicate the same and similar amino acids, respectively.

Fig. S3 Amino acid alignment of PsyR protein of different isolates of *P. syringae*.
Stop codons are indicated as red asterisks. Asterisks and dots below the sequences indicate the same and similar amino acids, respectively.

Fig. S4 Comparisons between DNA and amino acid sequences of *Pta*6605 and *Pto*DC3000.
Both 3'-ends of *psyI* and *psyR* and corresponding C-terminal regions of PsyI (red) and PsyR (blue) are shown. In *Pta*DC3000, deletion of one nucleotide caused a frame shift that eliminated the stop codon and extended the additional C-terminal sequence. Consequently, 69 bp of both ORF at 3' ends of *psyI* and *psyR* are overlapped in *Pto*DC3000.

Fig. S5 Comparisons of psyR DNA sequences and PsyR deduced amino acid sequences between *Pta*6605 (Pta) and *P. savastanoi* pv. *glycinea* KN44 (Pgl).
Both *psyR* DNA sequences are highly homologous each other at 99% identity, and identical nucleotides are indicated as asterisks. The nucleotides and amino acids of Pgl different from Pta is shown in red. Stop codons are also shown as red asterisks.

Fig. S6 DNA sequences of *rsmX*, *rsmY*, and *rsmZ* of *Pta*6605.
Upstream promoter regions and transcribed regions of five *rsmX* (A), *rsmY* (B), and *rsmZ* (C) are shown. The

consensus upstream activating sequence (UAS) (Humair et al. 2010), -35 and -10 promoter sites are indicated in red. Transcription start sites are indicated by arrows and shown as +1. The GGA motifs in the transcribed region are indicated by blue letters. The sequences highlighted in green are identical in all five *rsmX* genes and similar to the *rsmY* gene at their 3' end. These sequences are predicted to form a stem-loop, which functions as a rho-independent terminator. Underlined regions in *rsmX2* and *rsmY* were used as probes in Northern blot hybridization.

Table S1 Bacterial strains used in AHL assay.

Table S2 Gene expression profiles of high-density cells compared with those of low-density cells in *Pto*DC3000 by microarray analysis.

Table S3 Genes whose expressions were increased more than 2 times at high cell density than at low cell density.

Table S4 Genes whose expressions were decreased to less than half of the low cell density at high bacterial cell density.

Table 1 Bacterial strains used in this study

Bacterial strains	MAFF number	Abbreviation
P. amygdali pv. *tabaci* isolate 6605	-	*Pta*6605
P. amygdali pv. *tabaci* isolate 11528	-	*Pta*11528
P. amygdali pv. *lachrymans* YM7902	-	*Pla*YM7902
P. amygdali pv. *mellea* N6801	-	*Pme*N6801
P. amygdali pv. *morsprunorum* FTRS_U7805	-	*Pmo*FTRS
P. amygdali pv. *myricae* AZ84488	-	*Pmy*AZ84488
P. amygdali pv. *sesami* HC_1	-	*Pse*HC_1
P. savastanoi pv. *glycinea* BR1	210373	*Pgl*BR1
P. savastanoi pv. *glycinea* KN44	301683	*Pgl*KN44
P. savastanoi pv. *glycinea* LN10	210389	*Pgl*LN10
P. savastanoi pv. *phaseolicola* 1448A	-	*Pph*1448A
P. savastanoi pv. *phaseolicola* Y5-2	-	*Pph*Y5-2
P. syringae pv. *maculicola* H7608	301175	*Pma*H7608
P. syringae pv. *maculicola* KN91	302731	*Pma*KN91
P. syringae pv. *syringae* B728a	-	*Psy*B728a
P. syringae pv. *tomato* DC3000	-	*Pto*DC3000
P. syringae pv. *tomato* T1	-	*Pto*T1

Table 2 Oligonucleotides used for Northern blot hybridization

Oligonucleotide	Sequence
Pto rsmX2-R	AAAAAACCCGCCGAAGCGGGTGGTATTGCAACATGACCATTCCAACGTCCTGTCAGTAGCCTCCTGGCAATGGTCGATCG
Pto rsmY-R	AAAGAAAACCCCGCCTAAGCGGGGCTTTCCAGACTGTTTCCCTGATTTCCCTTTCACCCCGCCGTCCTGGCAGGCTTCCC
Pta rsmX2-R	AAAAAACCCGCCGAAGCGGGTGGTTTTGCAACATGACCATTCCGACATCCTGTCAGTAGCCTCCTGGCAATGGTCGATCT
Pta rsmY-R	AAAGAAAACCCCGCCGAAGCgGGGCTTTCCAGACTGTTTCCCTGATTTCCCtTTCACCCCAcCGTCCTGGCAGGCTTCCC

Each nucleotide is the complementary sequence of the corresponding small non-coding RNA, and covers 2/3 of the full size RNA.

Table 3 Gene expression profiles of small noncoding RNAs in high and low cell densities

Gene name	Product name	LCD	HCD	HCD/LCD
PSPTO_5671	*rsmX2*	0.64	36.22	56.73
PSPTO_5673	*rsmX3*	0.24	10.27	42.51
PSPTO_5674	*rsmX4*	0.44	15.24	34.53
PSPTO_5675	*rsmX5*	0.14	3.76	27.3
PSPTO_5647	*rsmY*	91.8	881.64	9.6
PSPTO_5672	*rsmX1*	10.21	95.12	9.31
PSPTO_5652	*rsmZ*	23.53	61.26	2.6

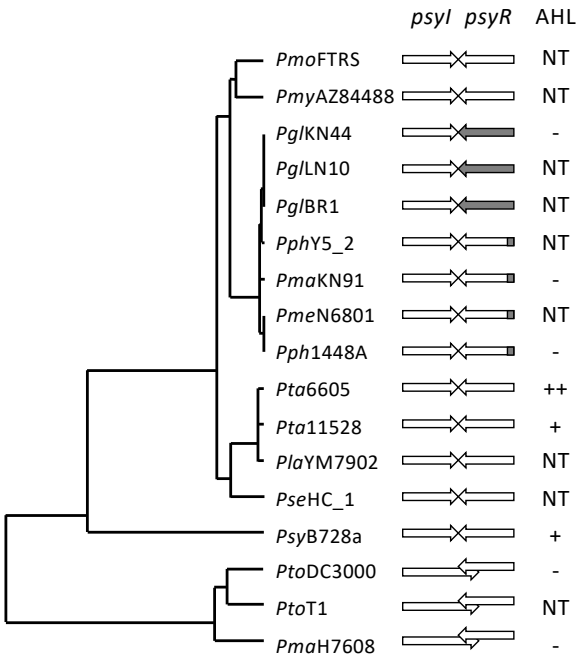

Fig. 1. Structure of quorum sensing genes, *psyI* and *psyR*, and production of *N*-acylhomoserine lactones in *Pseudomonas syringae* pathovars and isolates.
A phylogenetic tree of pathovars and isolates of *P*. *syringae* was constructed based on the sequence of *rpoD*. A gene for AHL synthase, *psyI*, and a gene for a transcriptional regulator, *psyR*, are transcribed convergently. Overlapping regions of two arrows indicate overlapping of two open reading frames. The dark portion in arrows of *psyR* indicates an untranslatable sequence by the stop codon(s) generated by the nucleotide substitution(s). The right column of AHL indicates the experimental result of AHL production. AHL detection is indicated as plus (+) and minus (-). NT: not tested.

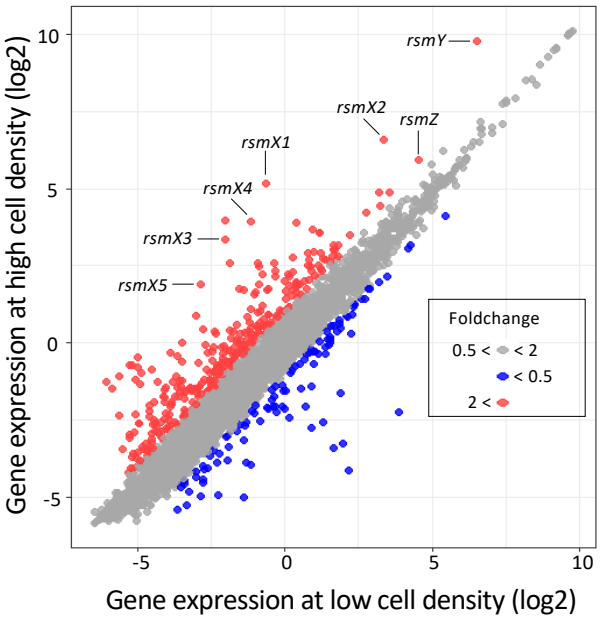

Fig. 2 Result of microarray analysis.
The open source R software (R version 3.2.5, http://www.r-project.org/) was used for microarray analysis and visualization. Genes expressed in *P. syringae* pv. *tomato* DC3000 at high cell density (OD_{600} = 1.0) and at low cell density (OD_{600} = 0.01) were plotted. Each dot represents individual level of gene expression. Red dots and blue dots indicate the genes expressed more than twice as much and less than half as much in high cell density conditions, respectively, whereas grey dots indicate the genes expressed more than half and less than twice as much. Five *rsmX*, *rsmY* and *rsmZ* genes are shown.

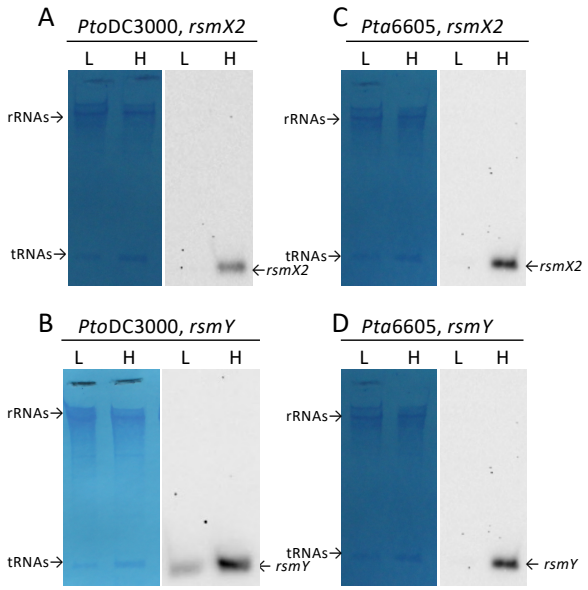

Fig. 3 Northern blot hybridization of *rsmX2* (A and C) and *rsmY* (B and D) of *Pto*DC3000 (A and B) and *Pta*6605 (C and D).
In each set of experiments, the methylene blue-stained membrane is shown on the left, and the corresponding hybridization result is shown on the right. Total RNAs (1 µg of *Pto*DC3000 and 0.5 µg of *Pta*6605) prepared from low-density cells (lane L, OD_{600} = 0.01) and high-density cells (lane H, OD_{600} = 1.0) were used for Northern blot hybridization. DIG-labeled oligonucleotides, Pto-rsmX2-R and Pto-rsmY-R, were used as hybridization probes for *Pto*DC3000, and Pta-rsmX2-R and Pta-rsmY-R for *Pta*6605, respectively.

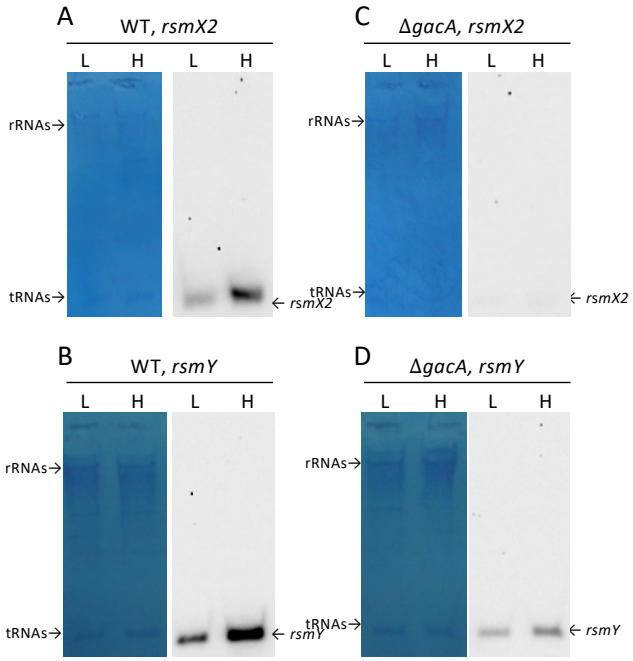

Fig. 4 Northern blot hybridization of *rsmX2* (A and C) and *rsmY* (B and D) of *Pta*6605 WT (A and B) and *Pta*6605Δ*gacA* (C and D).
In each set of experiments, the methylene blue-stained membrane is shown on the left, and the corresponding hybridization result is shown on the right. Total RNAs (1 µg of *Pta*6605) prepared from low-density cells (lane L, OD_{600} = 0.01) and high-density cells (lane H, OD_{600} = 1.0) were used for Northern blot hybridization. DIG-labeled oligonucleotides, Pta-rsmX2-R, and Pta-rsmY-R were used as hybridization probes for *Pta*6605.

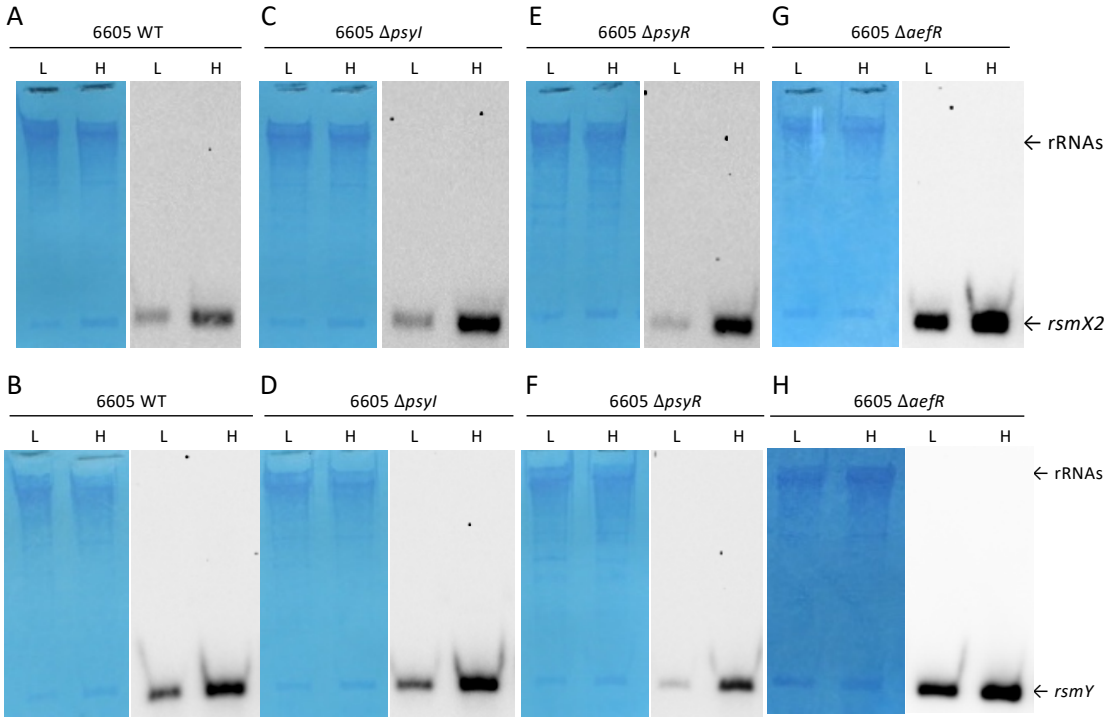

Fig. 5 Northern blot hybridization of *rsmX2* (A, C, E and G) and *rsmY* (B, D, F and H) of *Pta*6605 WT (A and B), *Pta*6605Δ*psyI* (C and D), *Pta*6605Δ*psyR* (E and F), and *Pta*6605Δ*aefR* (G and H).
In each set of experiments, the methylene blue-stained membrane is shown on the left, and the corresponding hybridization result is shown on the right. Total RNAs (1 µg of *Pta*6605) prepared from low-density cells (lane L, OD_{600} = 0.01) and high-density cells (lane H, OD_{600} = 1.0) were used for Northern blot hybridization. DIG-labeled oligonucleotides, Pta-rsmX2-R, and Pta-rsmY-R were used as hybridization probes for *Pta*6605.